ANTICANCER RESEARCH *37*: 2373-2379 (2017)
doi:10.21873/anticanres.11575

Inhibition of Importin β1 With a 2-Aminothiazole Derivative Resulted in G_2/M Cell-cycle Arrest and Apoptosis

SIYOUNG HA[1*], JAESUNG CHOI[2*], NA YOUNG MIN[2], KWANG-HO LEE[2] and SEUNG WOOK HAM[1]

[1]*Department of Chemistry, Chung-Ang University, Seoul, Republic of Korea;*
[2]*Department of Life Science, Chung-Ang University, Seoul, Republic of Korea*

Abstract. *Background: The design and synthesis of novel chemotherapeutic agents that can induce apoptosis and cell-cycle arrest has emerged as an attractive approach for the treatment of cancer, because they can limit possible nonspecific effects of compound treatment. Previous studies established that the expression of KPNB1 was increased in several cancer cells and transformed cell lines and inhibition of KPNB1 using siRNA significantly inhibited cervical tumour proliferation, but did not affect normal cervical epithelium. Recently, we reported that a KPNB1 inhibitor, the 2-aminothiazole derivative 1, possesses strong anti-proliferative effects against several cancer cells in the nanomolar concentration range. Results: Treatment with compound 1 interferes with cell-cycle progression in the G_2/M phase, as detected by flow cytometry analysis and results in apoptosis by the intrinsic pathway. Fluorescence microscopic analysis of mitotic cells predominantly mitotic abnormal cells with monopolar spindles and treatment with compound 1 did not affect polymerization of microtubules. Conclusion: Compound 1, as a KPNB1 inhibitor, might be a good target for future development of anticancer agents showing the activities of apoptosis and cell cycle arrest.*

Proteins produced in the cytoplasm are transported through nuclear pore complexes (NPCs) by carrier proteins known as importins (or karyopherins) to perform genetic and transcriptional functions in the nucleus (1). The first such transport protein identified, importin β1 (KPNB1), transports cargos into the nucleus with an adaptor protein such as KPNA (importin-α1) in the classical transport pathway (2-6), or in the non-classical transport pathway (7-10). Previous studies established that the expression of KPNB1 (11, 12) and the level of KPNB1 mRNA (13) are increased in several types of cancer cells and transformed cell lines. It has been reported that inhibition of KPNB1 using siRNA, achieves significant inhibition of cervical tumour proliferation, but does not affect normal cervical epithelium (11). Recently, we found that compound **1** possesses strong anti-proliferative effects against several types of cancer cells and exhibits strong binding affinity to KPNB1 (K_d: ~20 nM) (14). From molecular docking experiments, we also found that compound **1** binds strongly to KPNB1, in a pocket centered around serine-476.

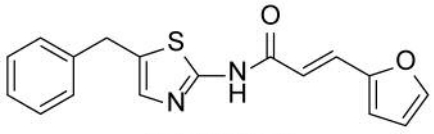

compound **1**

Components of the cell-cycle machinery are frequently altered in human cancer. Abnormal cells are eliminated by apoptosis, but cancer cells develop mechanisms to prevent this process, in the same way they manage to avoid cellular growth constraints. The ability of tumour cells to evade apoptosis can play a significant role in their resistance to conventional therapeutic regimens, therefore targeting apoptosis in cancer treatment would be beneficial. Previously, downregulation of KPNB1 by its siRNA was also shown to result in the induction of apoptosis and mitotic arrest in cervical cancer cells. However, KPNB1 has a large surface area, and it has inherent flexibility to interact with diverse proteins (15-20). We wondered whether binding of the small molecule, compound **1**, into the binding pocket would result in significant changes in the interaction between KPNB1 and certain cargo proteins related to apoptosis and cell cycle arrest. Therefore, the effects of compound **1** on apoptosis and cell-cycle arrest were determined in this study.

*Siyoung Ha and Jaesung Choi contributed equally to the writing of this article.

Correspondence to: Seung Wook Ham, Ph.D., Departments of Chemistry, Chung-Ang University, Seoul 156-756, Republic of Korea. Tel: +82 28205203, Fax: +82 28254736, e-mail: swham@cau.ac.kr

Key Words: KPNB1 inhibitor, 2-aminothiazole derivative, cell cycle, apoptosis, mitotic defects.

Table I. *IC_{50} values of compound 1 in various human cell lines. Flow cytometry analysis showed that the treatment with compound 1 resulted in a significant increase in the percentage of SK-OV3 and HeLa cells in G_2/M phase of the cell cycle in a dose- and time-dependent manner and an increase in the percentage of SubG1 peaks, indicating increased cell death.*

Time	Compound 1 (nM)	% cells in SK-OV3				% cells in HeLa			
		Sub-G_1	G_1	S	G_2/M	Sub-G_1	G_1	S	G_2/M
24 h	0	0.4	57.0	10.7	31.9	0.7	53.6	8.0	31.1
	50	0.1	58.1	8.6	28.7	3.7	42.5	7.9	38.4
	100	6.5	16.0	7.0	70.5	6.3	9.8	6.2	66.6
48 h	0	0.4	54.6	8.2	32.4	1.0	70.0	13.3	15.7
	50	7.4	30.9	15.4	38.6	10.4	56.6	15.7	17.3
	100	19.5	24.8	13.8	41.9	25.2	26.4	25.1	23.3

Materials and Methods

Cell culture and drug treatments. The HeLa human cervical cancer cell line was obtained from the Korean Cell Line Bank (Seoul, Korea) and cultured at 37˚C under a 5% CO_2 atmosphere in DMEM medium (Sigma Aldrich, St. Louis, MO, USA) supplemented with 10% fetal bovine serum (Young In Frontier, Seoul, Korea). The SK-OV3 and HeLa human cancer cell lines were obtained from Korean Cell Line Bank (Seoul, Korea) and cultured at 37˚C under a 5% CO_2 atmosphere in RPMI 1640 medium (WelGENE, Daegu, Korea) supplemented with 10% fetal bovine serum (WelGENE, Daegu, Korea). Twenty-four hours after seeding, compound 1 was added to the culture medium to a final concentration of 10 nM, 50 nM and 100 nM. Afterwards cells were incubated with compound 1 for various time points.

Western blot analysis. Cells were suspended in RIPA buffer (Tris-HCl [pH 8.0] 50 mM, NaCl 150 mM, SDS 0.1%, SDC 0.5%, NP-40 1%, EDTA 1 mM). Protein samples were separated through sodium dodecyl sulfate polyacrylamide gel electrophoresis and transferred to nitrocellulose membranes (Millipore, MA, USA). Membranes were blocked with 5% skim milk in tris-buffered saline with 0.1% Tween 20 (TBS-T). The primary antibodies against the target proteins were anti-caspase-3 mouse polyclonal IgG (Santa Cruz, CA, USA), anti caspase 8 mouse monoclonal IgG (Cell signaling technologies, MA, USA), anti caspase 9 rabbit polyclonal IgG (Cell signaling technologies, MA, USA), anti-bax rabbit polyclonal IgG (Santa Cruz, CA, USA), anti-bcl-2 mouse monoclonal IgG (Santa Cruz, CA, USA), anti-PARP rabbit polyclonal IgG (Santa Cruz, CA, USA) and anti-β-actin mouse monoclonal IgG (Sigma Aldrich, St. Louis, MO, USA); all antibodies were diluted in TBS-T (1:500~1:10000) and applied to membranes overnight at 4˚C. Secondary antibodies were diluted in TBS-T and applied to the membrane for 1 h at room temperature. Signals were visualized using enhanced chemiluminescence (ECL).

Flow cytometry assay. Cells were first harvested by trypsinization, then washed with cold DPBS, and fixed with 70% ethanol/DPBS at 4˚C overnight before harvesting. Cells were then permeabilized and labeled with 10 μg/ml propidium iodide (PI) (Sigma Aldrich, St. Louis, MO, USA). DNA contents were analyzed with a Navios flow cytometer (Beckman Coulter, CA, USA).

Fluorescent microscopy. Cells were grown on poly-D-lysine coated coverslips and treated with compound 1 or KPNB1 siRNA. Cells were fixed with cold methanol for 15 min and washed with PBS. Coverslips were subsequently incubated with anti-β-tubulin (1:100, Sigma-Aldrich, St. Louis, MO, USA) for 1 h and FITC-conjugated goat anti-mouse (1:100, Jackson ImmunoResearch, PA, USA) for 1 h. After each step, coverslips were washed three times with PBS. Nuclear DNA was stained using 10 ng/ml 4',6-diamidino-2-phenylindole (DAPI) for 15 min and washed with PBS. Coverslips were mounted with faramount (DAKO corporation, Hamburg, Germany) and images were acquired by means of a digital camera (DS-Qi1Mc, Nikon) and NIS-Elements image analysis software (Nikon Instruments Inc., USA).

Tubulin polymerization assay. The polymerization was determined in 100 μl volumes at 37˚C with the tubulin polymerization assay kit (Cytoskeleton, Denver, USA). Purified tubulin was >99% pure from bovine brain. Control sample was 5% DMSO in general tubulin buffer and all compounds were 10 μM of per well. Tubulin polymerization was monitored through measurements of the change in absorbance. They were measured at 30 sec intervals for 60 min using a Multi-Mode microplate reader (Bio-Tek Instruments, Highland Park, VT).

Results and Discussion

In order to investigate whether cell death induced from compound **1** was related to apoptosis, we determined apoptosis with Annexin V-FITC and propidium iodide solution (PI) by flow cytometry (Figure 1). The percentage of total apoptotic cells (early and late apoptotic cells) increased from 2.0% (control) to 9.7% (100 nM compound 1) for SK-OV3 cells, and 4.1 % (control) to 23.7% (100 nM compound 1) for HeLa cells at 24 h, showing that compound **1** induced apoptosis in a higher rate in HeLa cells than in SK-OV3 cells. However, we did not observe cells undergoing necrosis upon treatment with 100 nM compound **1**. In the intrinsic apoptotic pathway, anti-apoptotic Bcl-2 proteins are eliminated by cell death signals, which stimulate the release of cytochrome *c* from the mitochondrial intermembrane space

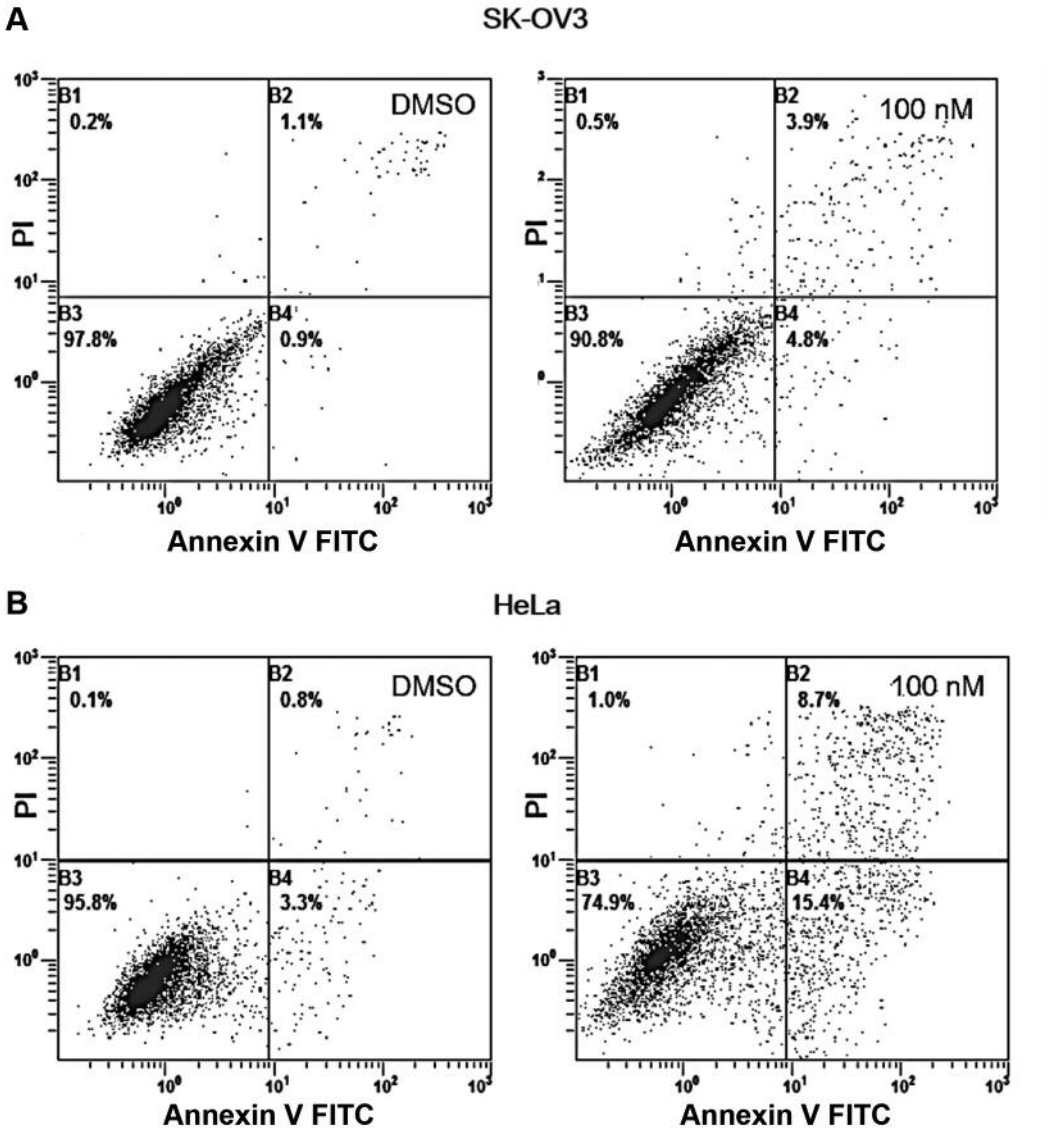

Figure 1. *Compound* ***1*** *induced cell apoptosis. SK-OV3 and HeLa cells were treated with 100 nM compound 1 for 24 h. Cells were then stained with Annexin V-FITC and propidium iodide (PI), and analyzed using flow cytometry. Four different cell populations are marked as follows: Live cell population (PI − AV−), early apoptosis (PI − AV+), late apoptosis (PI + AV+) and necrosis (PI + AV−). (A) Flow cytometry analysis of SK-OV3 cells. (B) Flow cytometry analysis of HeLa cells.*

to the cytosol by pro-apoptotic proteins, such as Bax (21). Cytochrome *c* then induces the activation of caspase 9 as the apical caspase. Caspase 9 further activates the effector caspase 3/7. A previous report demonstrated that inhibition of KPNB1 by its siRNA resulted in a sustained degradation of anti-apoptotic proteins, release of cytochrome *c*, and increase of caspases 3/7 activity in the intrinsic mitochondrial-dependent pathway of apoptosis (11). Therefore, we examined the cleaved activation of caspase 9, the upstream effector of caspase 3, as an indicator of the intrinsic pathway of apoptosis. Western blotting analysis demonstrated that caspase 9 cleavage was increased in a dose- and time-dependent manner when HeLa cells were treated with compound **1** (Figure 2). Another marker of apoptosis, PARP is a downstream substrate of the caspase family. Treatment resulted of compound **1** in significant dose- and time-dependent cleavage of full length PARP in cells, suggesting cell death *via* an apoptotic pathway. Moreover, treatment with compound **1** decreased the level of anti-apoptotic Bcl-2, further suggesting activation of intrinsic apoptosis.

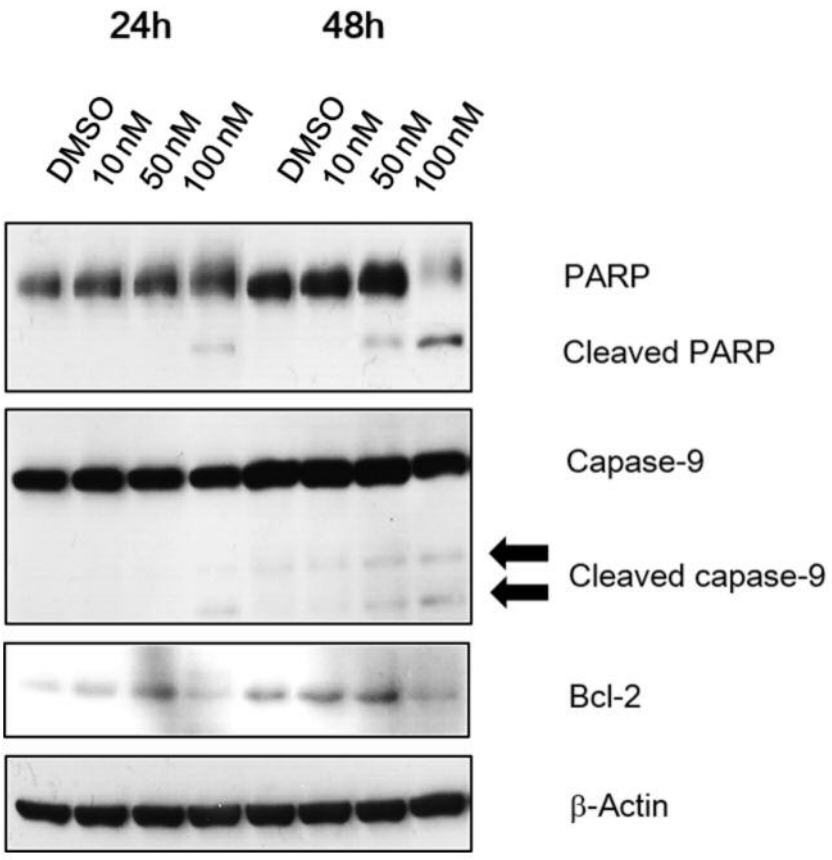

Figure 2. *Western blot analysis using anti-PARP, PARP, cleaved caspase 9, caspase 9, Bcl-2, and β-actin antibodies, after treating with different concentrations of compound 1 (10 nm, 50 nM, 100 nM) for 24 and 48 h. The results are representative of three independent experiments.*

In order to further determine whether compound 1 caused growth inhibition, we analyzed the cell cycles of SK-OV3 and HeLa treated for 24 and 48 h with compound 1 at 50 and 100 nM concentrations, using flow cytometry. As shown in Table I, the treatment with compound **1** resulted in a significant decrease in the percentage of both cell lines in G_1, and an associated significant increase in the percentage of cells in G_2/M phase of the cell cycle in a dose- and time-dependent manner. As expected, the percentage of SubG1 peaks increased from 0.4% (control) to 19.5 % for SK-OV3 cells, and from 1.0% (control) to 25.2 % for HeLa, indicating increased cell death. This observation is consistent with the findings that treatment with KPNB1 siRNA causes G_2/M phase arrest, followed by apoptosis in cervical cancer cells.

In addition to its roles in the nuclear transport pathway of cargos, it has been reported that KPNB1 is involved in both early and late mitotic events by affecting spindle assembly and nuclear envelope reassembly (22). Quantitative balance of KPNB1 and RanGTP is also required for mitotic spindle function. For example, treatment with importazole, a small-molecule inhibitor of the interaction between KPNB1 and RanGTP, caused dose-dependent defects in spindle assembly, spindle positioning, and chromosome alignment (23). It was also reported that knockdown of KPNB1 expression with siRNA in cancer cells produced mitotic defects, such as multipolar spindles, chromosome misalignment, and lagging chromosomes (11).

To compare the effects on mitotic progression of compound 1 treatment with the mitotic defects of KPNB1 knockdown, SK-OV3 cells were treated with either compound 1 or KPNB1 siRNA, and an immunofluorescence assay was performed. When cells were transfected with KPNB1 siRNA for 72 h, as shown in Figure 3E and F, immunofluorescence staining showed cells with four types of mitotic abnormalities: Astro-like monopolar spindles (35%), misalignment of chromosomes (45%), multipolar spindles (8%), and lagging chromosomes in anaphase/telophase (12%). Meanwhile, treatment with 100 nM of compound 1 resulted in an increase of mitotic cells (36.5%) (Figure 3B). From analysis of these mitotic cells with tubulin and DAPI staining, cells with monopolar spindles were predominantly observed (Figure 3D, 67%), while DMSO-

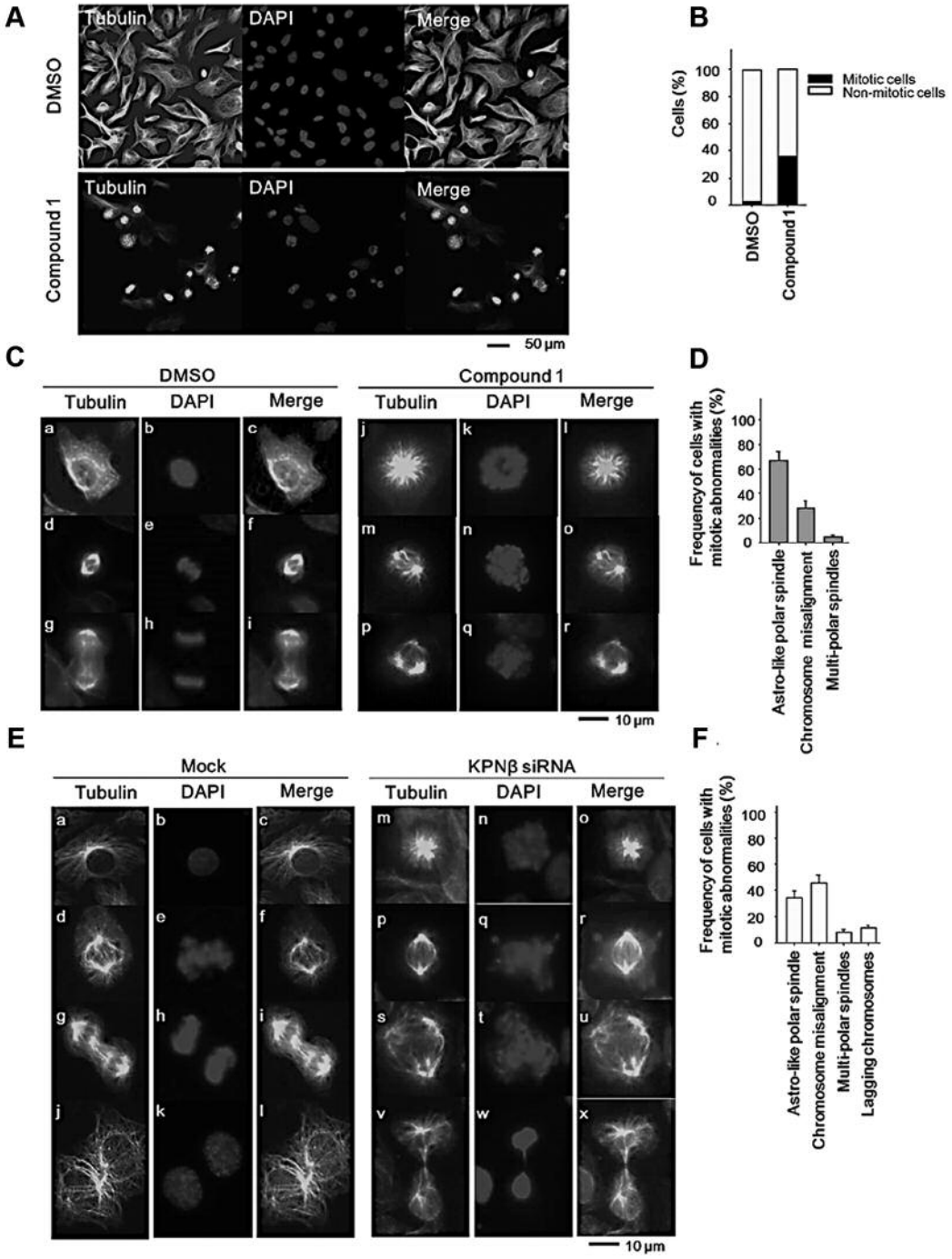

Figure 3. *Prolonged mitotic arrest and distinct mitotic defects of compound 1 and KPNB1 siRNA in SK-OV3 cells. (A) SK-OV3 cells were treated with 100 nM of compound* ***1*** *or DMSO for 24 h and β-tubulin immunofluorescence and DAPI fluorescence visualized. Size bar is 50 μm. (B) Mitotic cells were counted in compound* ***1****- and DMSO-treated cells. Cells were counted in triplicate, >150 cells per count. (C) Representative images are shown for mitotic abnormalities induced by DMSO and compound 1. In DMSO-treated SK-OV3, cells were normally dividing, as shown in images a-i. However, in compound* ***1****-treated cells, astro-like polar spindles (images j, k, l), dipolar spindles with chromosome misalignments (images m, n, o), and multipolar spindles (images p, q, r) were observed. Size bar is 10 μm. (D) The frequency of cells with mitotic abnormalities was determined, in triplicate, in >80 cells of the mitotic cell population in compound* ***1****-treated SK-OV3. (E) SK-OV3 cells were transfected with KPNB1 siRNA for 72 h and β-tubulin immunofluorescence and DAPI fluorescence visualized. Representative images are shown for mitotic abnormalities in mock and KPNB1 siRNA-treated cells. Astro-like polar spindles (images m, n, o), misalignment of chromosomes (images p, q, r), multipolar spindles (images s, t, u), and lagging chromosomes in anaphase/telophase (images v, w, x) were observed in KPNB1 siRNA-treated cells. (F) The frequency of cells with mitotic abnormalities was determined, in triplicate, in >150 cells of the mitotic cell population in KPNB1 siRNA-treated SK-OV3.*

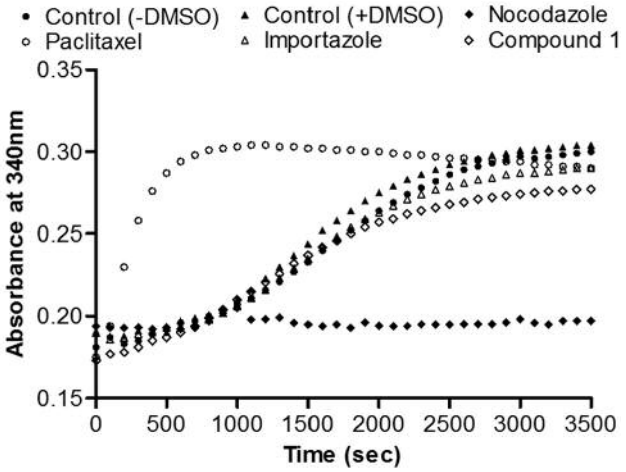

Figure 4. *Effect of compound **1** on microtubule polymerization in vitro. Bovine brain tubulin protein (3 mg/ml) was mixed with special reaction buffer as described in the Materials and Methods Section, and incubated with 10 μM solutions of each compound in DMSO and incubated with only DMSO and without DMSO as controls. The polymerization of tubulin was measured based on the increase in optical density. O.D. (340 nm) and was measured for every minute for a total of 40 min at 37˚C. Unlike paclitaxel and nocodazole, treatment with compound **1** and importazole in the cell-free system had no effect on tubulin density.*

treated SK-OV3 cells were found dividing normally (Figure 3C). Dipolar spindles with chromosome misalignments (28%) and multipolar spindles (5%) were also observed, but no lagging chromosomes in late mitosis were detected in cells treated with compound **1**.

Most antimitotic agents interact with microtubules. Monopolar spindles in mitotic cells, the most frequent defect caused by treatment with compound **1**, also observed in cells treated with antimicrotubule agents, such as nocodazole and monastrol, which interfere with the polymerization of microtubules (24, 25). Therefore, in order to compare the effect of compound **1** with other mitotic inhibitors, we investigated the effect of compound **1** on tubulin polymerization using an *in vitro* tubulin polymerization assay. While adding the microtubule-stabilizing agent, paclitaxel, into the reaction clearly increased polymerization of microtubules and the mitotic inhibitor, nocodazole, disrupted them, treatment with compound **1** did not affect polymerization of microtubules, as shown in Figure 4. This suggested that compound **1** does not bind directly to tubulin or microtubules. The tubulin polymerization assay also showed that importazole, an inhibitor of the KPNB1/RanGTP pathway, has no effect on tubulin density, which is consistent with the previous studies (23).

It has been reported that distinct domains of KPNB1 regulate diverse aspects of mitosis in human cells, including spindle pole formation, chromosome alignment, and mitotic progression (22). Regarding the types of mitotic abnormalities, the consequences of compound 1 on mitosis are somewhat different from those of KPNB1 knockdown from siRNA or RanGTP/KPNB1 inhibition with importazole. We have previously shown that the binding site for compound 1 is located on the concave face of H11 among 19 tandem HEAT repeats (termed H1-H19) (14). It is unclear whether the mitotic function of KPNB1 is inhibited by the significant changes in binding interaction that occur between KPNB1 and certain cargo proteins when compound **1** binds to this pocket.

In summary, treatment with compound **1** interferes with cell cycle progression in the G_2/M phase where KPNB1 has previously been reported to play a role. Treatment with compound 1 also results in apoptosis by the intrinsic pathway. The design and synthesis of novel chemotherapeutic agents that can induce apoptosis and cell cycle arrest have emerged as attractive approaches in cancer therapy because these agents can limit possible non-specific effects of compound treatment. Therefore, as a KPNB1 inhibitor, compound **1** might be a good target for future development of anticancer agents and for study of KPNB1 functions.

References

1 Nakielny S and Dreyfuss G: Transport of proteins and RNAs in and out of the nucleus. Cell *99(7)*: 677-690, 1999.
2 Gorlich D, Prehn S, Laskey RA and Hartmann E: Isolation of a protein that is essential for the first step of nuclear protein import. Cell *79(5)*: 767-778, 1994.
3 Adam EJ and Adam SA: Identification of cytosolic factors required for nuclear location sequence-mediated binding to the nuclear envelope. J Cell Biol *125(3)*: 547-555, 1994.
4 Radu A, Blobel G and Moore MS: Identification of a protein complex that is required for nuclear protein import and mediates docking of import substrate to distinct nucleoporins. Proc Natl Acad Sci USA *92(5)*: 1769-1773, 1995.
5 Harel A and Forbes DJ: Importin beta: conducting a much larger cellular symphony. Mol Cell *16(3)*: 319-330, 2004.
6 Lange A, Mills RE, Lange CJ, Stewart M, Devine SE and Corbett AH: Classical nuclear localization signals: definition, function, and interaction with importin alpha. J Biol Chem *282(8)*: 5101-5105, 2007.
7 Sakai J, Nohturfft A, Goldstein JL, Brown MS: Cleavage of sterol regulatory element-binding proteins (SREBPs) at site-1 requires interaction with SREBP cleavage-activating protein. Evidence from *in vivo* competition studies. J Biol Chem *273(10)*: 5785-5793, 1998.
8 Fagotto F, Gluck U and Gumbiner BM: Nuclear localization signal-independent and importin/karyopherin-independent nuclear import of beta-catenin. Curr Biol *8(4)*: 181-190, 1998.
9 Lam MH, Briggs LJ, Hu W, Martin TJ, Gillespie MT and Jans DA: Importin beta recognizes parathyroid hormone-related protein with high affinity and mediates its nuclear import in the absence of importin alpha. J Biol Chem *274(11)*: 7391-7398, 1999.
10 Hsu SC and Hung MC: Characterization of a novel tripartite nuclear localization sequence in the EGFR family. J Biol Chem *282(14)*: 10432-10440, 2007.

11 van der Watt PJ, Maske CP, Hendricks DT, Parker MI, Denny L, Govender D, Birrer MJ and Leaner VD: The Karyopherin proteins, Crm1 and Karyopherin beta1, are overexpressed in cervical cancer and are critical for cancer cell survival and proliferation. Int J Cancer *124(8)*: 1829-1840, 2009.
12 Yan W, Li R, He J, Du J and Hou J: Importin β1 mediates nuclear factor-κB signal transduction into the nuclei of myeloma cells and affects their proliferation and apoptosis. Cell Signal *27(4)*: 851-859, 2015.
13 Smith ER. Cai KQ, Smedberg JL, Ribeiro MM, Rula ME, Slater C, Godwin AK and Xu XX: Nuclear entry of activated MAPK is restricted in primary ovarian and mammary epithelial cells. PLoS One *5(2)*: e9295, 2010.
14 Kim YH, Ha S, Kim J and Ham SW: Identification of KPNB1 as a cellular target of aminothiazole derivatives with anticancer activity. ChemMedChem *11(13)*: 1406-1409, 2016.
15 Cingolani G, Petosa C, Weis K and Müller CW: Structure of importin-beta bound to the IBB domain of importin-alpha. Nature *399(6733)*: 221-229, 1999.
16 Vetter IR, Arndt A, Kutay U, Gorlich D and Wittinghofer A: Structural view of the Ran-Importin beta interaction at 2.3 A resolution. Cell *97(5)*: 635-646, 1999.
17 Chook YM and Blobel G: Structure of the nuclear transport complex karyopherin-beta2-Ran x GppNHp. Nature *399(6733)*: *399*: 230-237, 1999.
18 Lee SJ, Sekimoto T, Yamashita E, Nagoshi E, Nakagawa A, Imamoto N, Yoshimura M, Sakai H, Chong KT, Tsukihara T and Yoneda Y: The structure of importin-beta bound to SREBP-2: nuclear import of a transcription factor. Science *302(5650)*: 1571-1575, 2003.
19 Lee SJ, Matsuura Y, Liu SM and Stewart M: Structural basis for nuclear import complex dissociation by RanGTP. Nature *435(7042)*: 693-696, 2005.
20 Forwood JK, Lange A. Zachariae U, Marfori M, Preast C, Grubmuller H, Stewart M, Corbett AH and Kobe B: Quantitative structural analysis of importin-β flexibility: paradigm for solenoid protein structures. Structure *18(9)*: 1171-1183, 2010.
21 Elmore S. Apoptosis: a review of programmed cell death. Toxicol Pathol *35(4)*: 495-516, 2007.
22 Roscioli E, Di Francesco L, Bolognesi A, Giubettini M, Orlando S, Harel A, Schininà ME and Lavia P: Importin-β negatively regulates multiple aspects of mitosis including RANGAP1 recruitment to kinetochores. J Cell Biol *196(4)*: 435-450, 2012.
23 Soderholm JF, Bird SL, Kalab P, Sampathkumar Y, Hasegawa K, Uehara-Bingen M, Weis K and Heald R: Importazole, a small molecule inhibitor of the transport receptor importin-β. ACS Chem Biol *6(7)*: 700-708, 2011.
24 Steen JA, Steen H, Georgi A, Parker K, Springer M., Kirchner M, Hamprecht F and Kirschner MW: Different phosphorylation states of the anaphase promoting complex in response to antimitotic drugs: a quantitative proteomic analysis. Proc Natl Acad Sci USA *105(16)*: 6069-6074, 2008.
25 Choi HJ, Fukui M and Zhu BT: Role of cyclin B1/Cdc2 up-regulation in the development of mitotic prometaphase arrest in human breast cancer cells treated with nocodazole. PLoS One *6(8)*: e24312, 2011.

Received March 21, 2017
Revised April 6, 2017
Accepted April 7, 2017